STABILIZATION OF QUADCOPTER BY NESTED SATURATION FEEDBACK AND CONTROABILITY ANALYSIS

by

SIZHE ZHU

Submitted in partial fulfillment of the requirements for the degree

of Master of Science

Department of Systems and Control Engineering

CASE WESTERN RESERVE UNIVERSITY

August 2022

CASE WESTERN RESERVE UNIVERSITY SCHOOL OF GRADUATE STUDIES

We hereby approve the thesis/dissertation of

SIZHE ZHU

candidate for the degree of **Master of Science**.

Committee Chair

Prof. Wei Lin

Committee Member

Prof. Kenneth A. Loparo

Committee Member

Prof. Vira Chankong

Date of Defense

June 3, 2022

*We also certify that written approval has been obtained for any proprietary material contained therein.

Contents

Figures

Tables

Symbols

Name	Definition	Unit
g	Gravitational acceleration, -9.81	m/s^2
x,y,z	Position of center of quadcopter with respect to inertial frame	m
ψ,θ,ϕ	Euler angles (Yaw, Pitch, Roll)	rad
x_B,y_B,z_B	Axes of the body frame	
x_E,y_E,z_E	Axes of the inertial frame	
ω_i	Angular speed of motor i, i = 1,2,3,4	rad/s
f_i	Thrust force of motor i, 1 = 1.2.3.4	N
m	Mass of quadcopter	kg
J	Inertia matrix of the full rotational kinetic energy	
W_η	Transformation matrix	
R	Rotation matrix from body frame to inertial frame	
Q	Generalized coordinates for quadcopter	
ξ	Translational coordinates	
η	Rotational coordinates	
V_B	Linear velocity in body frame	m/s
v	Angular velocity	rad/s
l	Distance between center of mass to end of arm	m
F_ξ	The force act on the inertial frame	N
$\tilde{F}$	The force act on the body frame	N
τ	The generalized moment from generalized coordinates	NxM

Acknowledgements

First I want to express my appreciation to my research advisor Wei Lin. In these two years he taught and guided me in the way of doing research. Meanwhile I want to thank the Ph.D. in our lab Yuanjiu Wang and Jiwei Sun. They provided a lot of help and innovations to me when I had difficulties not only in the research and study but also in the daily life. In the end, I would also thank for my parents for their supports and inspiration in these years. And thank for them to support my thought of pursing Ph.D. Degree in the future.

Stabilization of Quadcopter by Nested Saturation Feedback and Controllability Analysis

Abstract

by

SIZHE ZHU

Quadcopter, also known as a drone, rotorcraft, or quadrotor, is a small-scale UAV used for various applications like photography, inspection, etc. Its composition contains two parts: reliable hardware and an effective control algorithm. To maximize its performance, developing a reliable control algorithm is essential. Also, while the quadcopter is facing the propellers failure, a proper solution for maintaining its stability is necessary.

In this thesis, the proposed controller is designed based on Lyapunov analysis using a nested saturation algorithm. First, the dynamic model of the four-rotor quadcopter is obtained via a Lagrange approach. Then the proposed controller is designed, and a global stability analysis of the closed-loop system is presented. Next, the MATLAB simulations show that the controller can autonomously perform flying experiments of taking off and hovering. In the second part, the periodic solutions and equilibria for the situations that quadcopter lost one and two (opposing) propellers are introduced.

Keywords: Quadcopter, UAV, Nested saturation feedback, Dynamic model, Propeller lost, Periodic solution, Equilibria

1 Introduction

1.1 Overview of Quadcopter

The quadcopter is a unique type of Unmanned Aerial Vehicle (UAV), which has Vertical Take-Off and Landing (VTOL) ability. Due to its inherently dynamic nature, the quadcopter has an advantage of maneuverability [1]. Nowadays, the small-scaled UAVs like a quadcopter are gaining top interest and popularity because:

- They are a powerful tool for scientific research due to their low cost, high maneuverability, and easy maintenance. Significant progress in various research areas (e.g., dynamics modeling, flight control, tracking, and navigation) have been made.
- They can be implemented in many applications, including emergency monitoring, search and rescue, geological survey, weather forecast, fire detection, and radiation monitoring [2].

One of the significant advantages of the unmanned flying vehicle is its flexibility and agility. For example, four rotors could provide stronger maneuverability and robustness than one or two rotors like the helicopter. Also, with some specific design and control, the quadcopter can hover and land while its losses one or even two propellers. On the other hand, like all other UAVs, the quadcopter has a lower risk of pilot casualties because the onboard pilots are not required, so operation errors can hardly affect them. Therefore, the quadcopters can be used for dangerous flying tasks such as searching

disaster scenes. Moreover, the fuel and maintenance cost is considerably lower than the traditional flying vehicles.

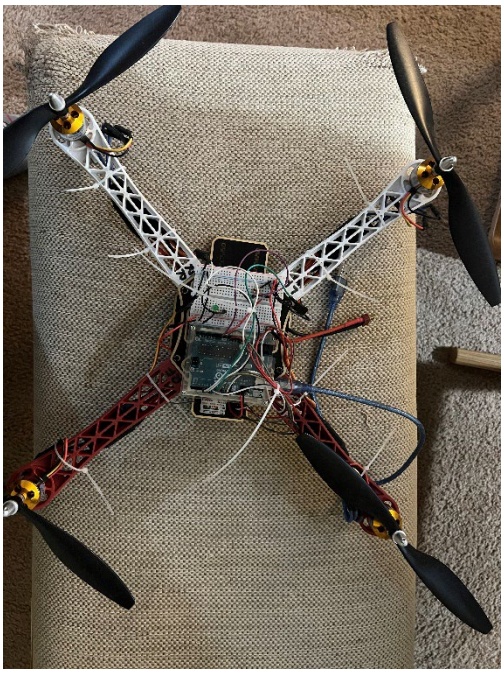

Figure 1.1 My self-made quadcopter

A quadcopter consists of a frame, rotors, central control chip, sensors, transmitter, and receiver. Moreover, a vision system could also be attached to the quadcopter. The frame is usually made of slim materials such as plastic or carbon fiber with greater intensity but lower weight. The structure of the frame varies depending on their flight mission and payload. For the motor part, the DC brushless motors are commonly used. And the rotation is driven by electronic speed control (ESC) circuits with PMW signals. The diagonal pair of propellers shares the same rotational direction. For example, the right front and left rear propellers rotate counterclockwise, right rear and left front propellers to rotate clockwise. The central control chip is the core part of executing the control algorithm. Nowadays, technology develops fast. Therefore, a simple device such as Arduino can fully meet all the requirements. For the sensor part, the inertial measurement

unit (IMU), which contains the accelerometer and gyroscope, provides the attitude and rotation of the quadcopter [1]. In addition, the GPS module and barometer will be added for tracking purposes to collect the position data. These are the necessary measurement for the flight control system. In the end, the receiver and transmitter are required to receive the real-time data and send operation signals.

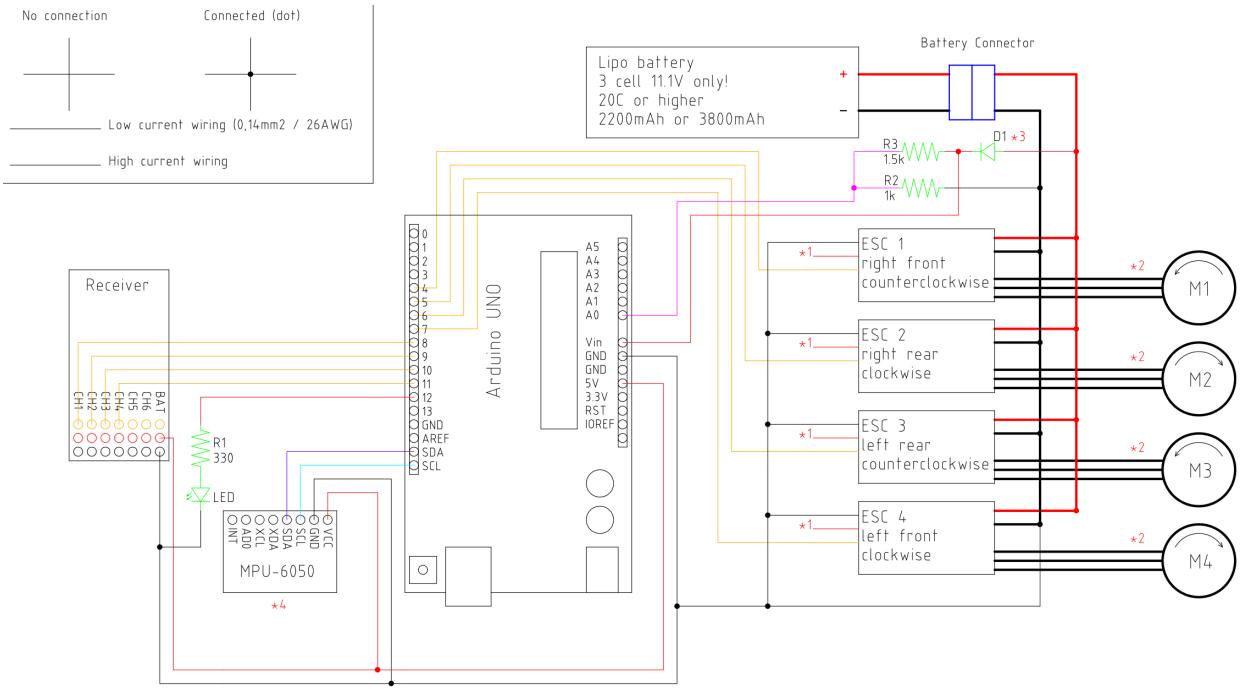

Figure 1.2 A example of quadcopter schematic

Therefore, due to the value of quadcopter applications, it is worthwhile to improve its performance. In recent studies, most of them focused on designing different physical structures so that the quadcopter can have more degrees of freedom. However, the discovery and development of new methods other than the classic PID control are also considerable.

1.2 Recent Studies of Quadcopter

The first quadcopter was designed in the 1920s. And after more than a hundred years of development, it has already become a standardized product that everyone can buy online for entertainment. For example, the smallest quadcopter from the well-known company DJIA is only about 50g. However, its battery can last 13 minutes flying. Users can attach the smartphone with the remote controller and connect to the drone's WIFI to fully control the quadcopter. Also, this drone can provide real time 720p HD transmission and give up to 5 MP photo quality. Furthermore, the drone can hover in the air steadily without shacking and vibration. Also, it can respond to users' remote control with ignorable time delay. By all means, the quadcopter has been well developed, and the stability technique is very mature.

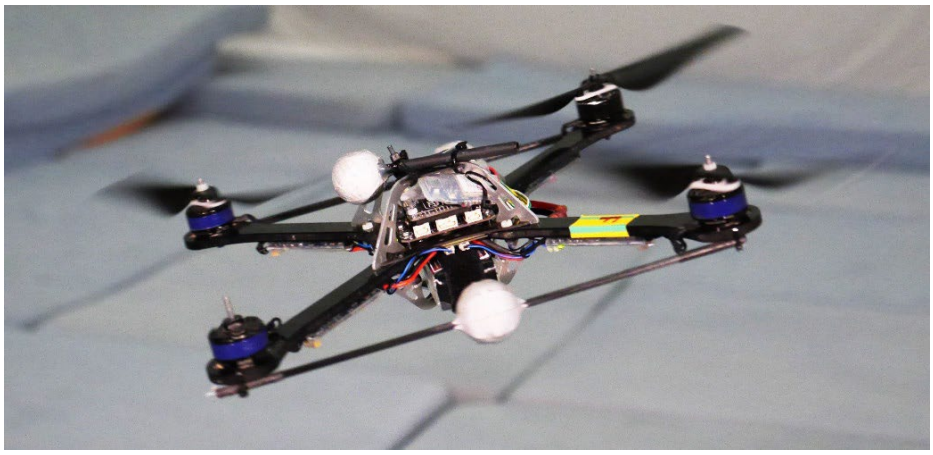

Figure 1.3 Quadcopter in controlled with one propeller lost [3]

In recent years, the solution with quadcopter loss propellers has been discovered. In the case of one lost propeller, letting the pair of functional opposing propellers produce equal thrust and choose an adaptive ratio between the third propeller and the pairs, the quadcopter can still be stabilized and hover in an ellipse trajectory [3]. However, there is

no solution for the cases when there are two adjacent propellers, or three propellers disabled.

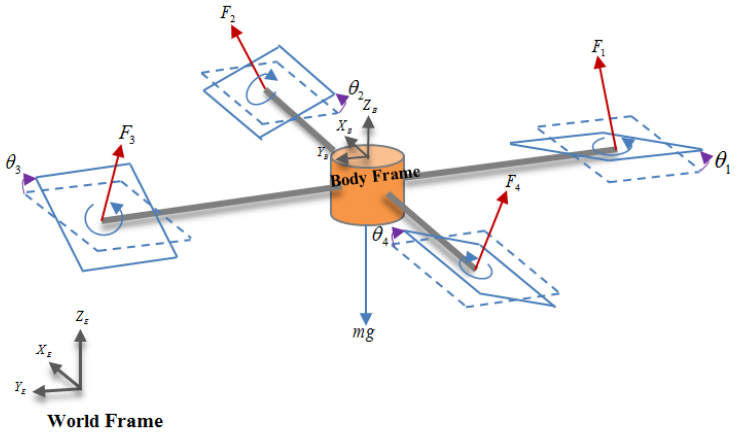

Figure 1.4 Coordinate frames and free body diagram of tilting quadcopter [4]

In another study, the researcher developed a slightly different physical structure of quadcopter, which can provide two more degrees of freedom, could significantly improve quadcopter's performance. The design is accomplished by using an additional motor for each rotor that enables the rotor to rotate along the axis of the quadcopter arm. Moreover, it turns the traditional quadcopter into an over-actuated flying vehicle allowing people to have complete control over its position and orientation [4]. This design has the potential to deal with the case when the quadcopter losses a pair of opposite propellers.

The adaptive control method is vital for dealing with the case when there are unknown parameters in a study. In recent years, several researchers have tried to implement adaptive control methodology into quadcopter research because they believe the equipment measurement error or high order nonlinearity terms could impact performance. However, the typical results of these studies are not capable of showing adaptive control method can perform well in quadcopter control.

1.3 Current Control Strategies

A traditional quadcopter is driven by four fixed propellers as actuators and six degrees of freedom to control. Therefore it is a naturally unstable underactuated system because it has more degrees of freedom than actuators. Therefore, the underactuated mechanical systems required fundamental nonlinear approaches. In recent years, there are many control techniques have been developed, such as PID control [6], backstepping control [7], adaptive control [5], and so on. Some have been proven to be efficient for dealing with quadcopter stabilization problems and trajectory tracking problems. However, the PID control technique is the most robust and most effective method for quadcopter control for now.

This thesis introduces a nested saturation control method based on Lozano's (2004) paper [8]. First, a generalized model will be developed based on the Euler Lagrange equations approach in chapter 2. Next, in chapter 3, a review of Lozano's result and why the method is reasonable and practical will be explained. Also, a discussion of saturation control with slight input delay will be presented in chapter 4, with how it deals with the rigid body robustness and parameter uncertainty. In the last part, we will discuss the possibility of implementing nested saturation design ideas to other UAVs.

2 Dynamic Modeling of Quadcopter

2.1 Mechanism of Quadcopter

A typical quadcopter is driven by four rotors on each arm of the frame as it showed in figure 1.1. However, there on two different configurations (understand as shape “x” or shape “+”) based on the definition of the body frame. Since the “x” configuration is more stable, in this case, we choose this one for the discussion.

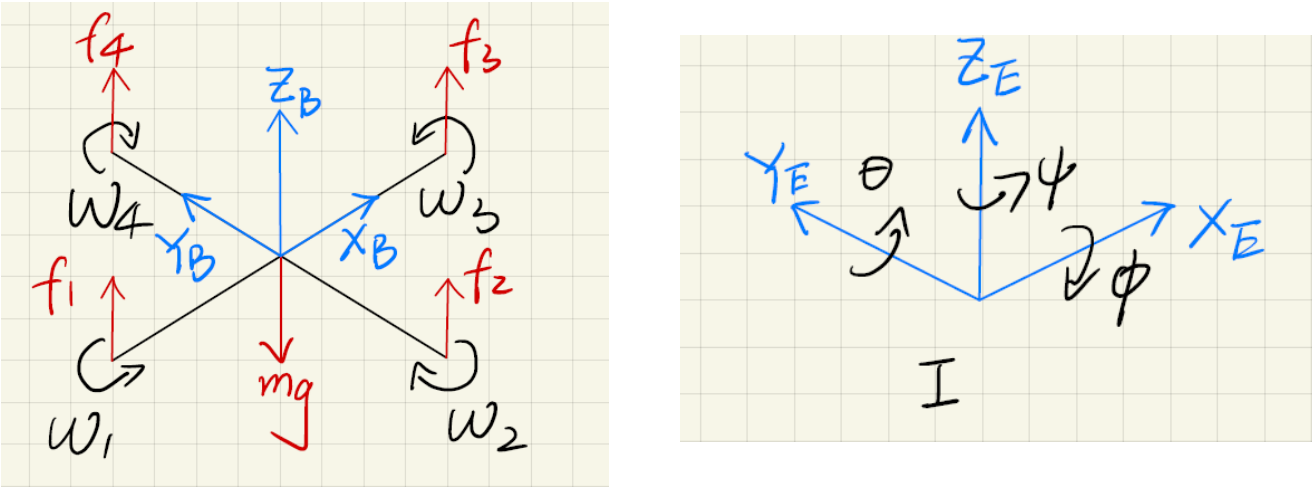

Figure 2.1 Quadcopter structure, Body frame (left), Inertial frame (Right)

The rotors are marked as 1,2,3,4. Rotor 1 and 3 are a pair of diagonal or opposite rotors that rotate counterclockwise, while the other pair is clockwise. All the propellers generated the upward thrust force to lift the quadcopter. The attitude of the quadcopter can be changed by changing the rotor speed. Also, by assigning the rotating speed of each propeller separately, we can configure four control inputs as total thrust and torque about x,y,z axis on the body frame of the quadcopter.

2.2 Frame Definition

2.2.1 Introduction of Inertial Frame and Body Frame

The body frame and inertial frame is presented in Figure 2.1.

The body frame is fixed on the quadcopter and the origin is in the center of quadcopter while z axis z_B is pointing vertically upward from the origin and x axis x_B is pointing rotor 3.

The inertial frame, or named as earth frame, is the absolute position with respect to the earth. Its origin is fixed on the earth surface or a specific preset point in 3D space and z_E is vertical to the ground.

Based on these two frames, we can define a generalized coordinates for the quadcopter:

$$Q = (x, y, z, \psi, \theta, \phi) \in R^6 \quad (2.1)$$

Which contains translational coordinates:

$$\xi = (x, y, z) \in R^3 \quad (2.2)$$

And rotational coordinates:

$$\eta = (\psi, \theta, \phi) \in R^3 \quad (2.3)$$

The translational coordinates show the position of quadcopter with respect to the inertial frame. The attitude coordinates is defined by Euler angles. Yaw angle ψ refers the rotation angle around z_E. Roll angle ϕ determines the rotation around x_E. And the pitch angle θ is the rotation angle around y_E.

2.2.2 Rotation Matrix and Transformation Matrix

The rotation matrix is a generalized matrix which is commonly been used in derivation of dynamic model for describing the orientation of the body frame with respect to the inertial frame.

It is commonly defined as:

$$R = \begin{pmatrix} \cos\theta\cos\psi & \sin\psi\sin\theta & -\sin\theta \\ \cos\psi\sin\theta\sin\phi - \sin\psi\cos\phi & \sin\psi\sin\theta\sin\phi + \cos\psi\cos\phi & \cos\theta\sin\phi \\ \cos\psi\sin\theta\cos\phi + \sin\psi\sin\phi & \sin\psi\sin\theta\cos\phi - \cos\psi\sin\phi & \cos\theta\cos\phi \end{pmatrix} \quad (2.4)$$

And $R^{-1} = R^T$.

The transformation matrix is defined as:

$$W_\eta = \begin{bmatrix} 1 & 0 & -\sin\theta \\ 0 & \cos\theta & \cos\theta\sin\phi \\ 0 & -\sin\phi & \cos\theta\cos\phi \end{bmatrix} \quad (2.5)$$

2.2.3 Linear Velocity and Angular Velocity

In the body frame, the linear velocity is determined by V_B and the angular velocity by v:

$$V_B = \begin{bmatrix} V_{x,B} \\ V_{y,B} \\ V_{z,B} \end{bmatrix} \quad (2.6)$$

$$v_B = \begin{bmatrix} p \\ q \\ r \end{bmatrix} \quad (2.7)$$

The relationship between angular velocity and rotation angles can be found as

$$\dot{\eta} = W_{\eta}^{-1} v_B \rightarrow \begin{bmatrix} \dot{\phi} \\ \dot{\theta} \\ \dot{\psi} \end{bmatrix} = \begin{bmatrix} 1 & \sin\theta \tan\theta & \cos\phi \tan\theta \\ 0 & \cos\theta & -\sin\phi \\ 0 & \sin\phi/\cos\theta & \cos\phi/\cos\theta \end{bmatrix} \begin{bmatrix} p \\ q \\ r \end{bmatrix} \quad (2.8)$$

$$v_B = W_{\eta} \dot{\eta} \rightarrow \begin{bmatrix} p \\ q \\ r \end{bmatrix} = \begin{bmatrix} 1 & 0 & -\sin\theta \\ 0 & \cos\theta & \cos\theta \sin\phi \\ 0 & -\sin\phi & \cos\theta \cos\phi \end{bmatrix} \begin{bmatrix} \dot{\phi} \\ \dot{\theta} \\ \dot{\psi} \end{bmatrix} \quad (2.9)$$

2.3 Derivation of Dynamic Model

2.3.1 Inertial Matrix J and I

The quadcopter is assumed to have symmetric structure with four arms aligned with the body x and y axes. Thus, the inertia matrix I is a diagonal matrix I in which I_{xx}=I_{yy}.

$$I = \begin{bmatrix} I_{xx} & 0 & 0 \\ 0 & I_{yy} & 0 \\ 0 & 0 & I_{zz} \end{bmatrix} \quad (2.10)$$

The matrix J acts as the inertia matrix for the full-rotational kinetic energy of the quadcopter expressed directly in terms of the generalized coordinates η [8]. These two inertia matrix can be transformed by the transformation matrix.

And the relationship between J and I is:

$$J = {w_{\eta}}^{T} I w_{\eta} =$$

$$\begin{bmatrix} I_{xx} & 0 & -I_{xx}\sin\theta \\ 0 & I_{yy}(\cos\theta)^2 + I_{zz}(\sin\phi)^2 & \left(I_{yy} - I_{zz}\right)\cos\phi \sin\phi \cos\theta \\ -I_{xx}\sin\theta & \left(I_{yy} - I_{zz}\right)\cos\phi \sin\phi \cos\theta & I_{xx}(\sin\theta)^2 + I_{yy}(\sin\phi)^2(\cos\theta)^2 + I_{zz}(\cos\phi)^2(\cos\theta)^2 \end{bmatrix}$$

(2.11)

2.3.2 Euler Lagrange Equation

Based on the translational and rotational coordinates we defined, we can get the translational kinetic energy and rotational kinetic energy of the quadcopter

$$T_{translational} \triangleq \frac{m}{2}\dot{\xi}^T\dot{\xi} \quad (2.12)$$

$$T_{rotational} \triangleq \frac{1}{2}\dot{\eta}^T J\dot{\eta} \quad (2.13)$$

The only potential energy we have to consider is the standard gravitational potential:

$$P = mgz \quad (2.14)$$

And based on the Lagrangian equation, we can have:

$$L(q,\dot{q}) = T_{transtional} + T_{rotational} - P = \frac{m}{2}\dot{\xi}^T\dot{\xi} + \frac{1}{2}\dot{\eta}^T J\dot{\eta} - mgz \quad (2.15)$$

Euler-Lagrange equation with external generalized force:

$$\frac{d}{dt}\frac{\partial L}{\partial \dot{q}} - \frac{\partial L}{\partial q} = F \quad (2.16)$$

$$F = (F_\xi, \tau) \quad (2.17)$$

Where τ is the generalized moment from generalized coordinates and F_ξ is the translational force applied to the quadcopter due to the control input. And

$$F_\xi = R\tilde{F} \quad (2.18)$$

$$\tilde{F} = \begin{pmatrix} 0 \\ 0 \\ u \end{pmatrix} \quad (2.19)$$

$$u_f = f_1 + f_2 + f_3 + f_4 \quad (2.20)$$

f_i, i = 1,2,3,4 is the thrust force of each rotor with

$$f_i = k_f \omega_i^2, i = 1,2,3,4 \qquad (2.21)$$

Where $k_f > 0$ is a constant and ω_i is the angular speed of motor "i".

$\tilde{F}$ is the force act on the body frame and when it times rotation matrix, we get F_ξ which is the force act on the spatial frame.

$$\tau \triangleq \begin{pmatrix} \tau_\psi \\ \tau_\theta \\ \tau_\phi \end{pmatrix} = \begin{pmatrix} \sum_{i=1}^{4} \tau_{M_i} \\ (f_2 - f_4)l \\ (f_3 - f_1)l \end{pmatrix} \qquad (2.22)$$

Where τ_{M_i} is the torque generated by each rotor. And l is the distance between center of mass to the motor.

2.3.3 Change of Coordinate and Further Simplification

Since there is no cross term combining in $\dot{\xi} and\ \dot{\eta}$ in equation (2.15), we can rewrite the Euler-Lagrange equation as

$$m\ddot{\xi} + \begin{pmatrix} 0 \\ 0 \\ mg \end{pmatrix} = F_\xi \qquad (2.23)$$

$$J\ddot{\eta} + \dot{J}\dot{\eta} - \frac{1}{2}\frac{\partial}{\partial \eta}(\dot{\eta}^T J \dot{\eta}) = \tau \qquad (2.24)$$

The Coriolis-Centripetal vector is defined as

$$\bar{V}(\eta, \dot{\eta}) = \dot{J}\dot{\eta} - \frac{1}{2}\frac{\partial}{\partial \eta}(\dot{\eta}^T J \dot{\eta}) = \left(\dot{J} - \frac{1}{2}\frac{\partial}{\partial \eta}(\dot{\eta}^T J)\right)\dot{\eta} = C(\eta, \dot{\eta})\dot{\eta} \qquad (2.25)$$

Then we can rewrite equation (2.23) and (2.24) as

$$m\ddot{\xi} = u\begin{pmatrix} -\sin\theta \\ \cos\theta \sin\theta \\ \cos\theta \cos\phi \end{pmatrix} + \begin{pmatrix} 0 \\ 0 \\ -mg \end{pmatrix} \quad (2.26)$$

$$J\ddot{\eta} = \tau - C(\eta, \dot{\eta})\dot{\eta} \quad (2.27)$$

To get rid of Coriolis term, we have to change the coordinate

$$\tau = C(\eta, \dot{\eta})\dot{\eta} + J\tilde{\tau} \quad (2.28)$$

And the new input $\tilde{\tau} = \begin{pmatrix} \tilde{\tau}_\psi \\ \tilde{\tau}_\theta \\ \tilde{\tau}_\phi \end{pmatrix} = \ddot{\eta}$.

2.3.4 Definition of State Variables and Control Inputs

Therefore from all the simplification, the equation (2.26) and (2.27) can be rewritten as

$$m\ddot{x} = -u\sin\theta \quad (2.29)$$

$$m\ddot{y} = u\cos\theta\sin\phi \quad (2.30)$$

$$m\ddot{z} = u\cos\theta\cos\phi - mg \quad (2.31)$$

$$\ddot{\psi} = \tilde{\tau}_{\psi} \quad (2.32)$$

$$\ddot{\theta} = \tilde{\tau}_{\theta} \quad (2.33)$$

$$\ddot{\phi} = \tilde{\tau}_{\phi} \quad (2.34)$$

The four control inputs $u, \tilde{\tau}_{\psi}, \tilde{\tau}_{\theta}, \tilde{\tau}_{\phi}$ are the total thrust or collective input and the new angular moments (yawing moment, pitching moment and rolling moment). And by figuring out the values of these control signals, the corresponding rotating speed of the four rotors can be calculated as well. And now we defined 12 state variables as

$$x_1 = x$$

$$x_2 = \dot{x}$$

$$x_3 = y$$

$$x_4 = \dot{y}$$

$$x_5 = z$$

$$x_6 = \dot{z}$$

$$x_7 = \psi$$

$$x_8 = \dot{\psi}$$

$$x_9 = \theta$$

$$x_{10} = \dot{\theta}$$

$$x_{11} = \phi$$

$$x_{12} = \dot{\phi}$$

(2.35)

By substitute the state variables and control inputs, we can get the generalized state space model for the quadcopter:

$$\dot{x_1} = x_2$$

$$\dot{x_2} = -\frac{u}{m}\sin x_9$$

$$\dot{x_3} = x_4$$

$$\dot{x_4} = \frac{u}{m}\cos x_9 \sin x_{11}$$

$$\dot{x_5} = x_6$$

$$\dot{x_6} = \frac{u}{m}\cos x_9 \cos x_{11} - g$$

$$\dot{x_7} = x_8$$

$$\dot{x_8} = \tilde{\tau}_\psi$$

$$\dot{x_9} = x_{10}$$

$$\dot{x_{10}} = \tilde{\tau}_\theta$$

$$\dot{x_{11}} = x_{12}$$

$$\dot{x_{12}} = \tilde{\tau}_\phi$$

(2.36)

3 Nested Saturation Design for Quadcopter Stabilization

3.1 Introduction of Nested Saturation Control

The controller based on Lyapunov analysis using a nested saturation algorithm is presented. The key idea is to transform the stabilization problem into the planar vertical take off and landing (PVTOL) aircraft problem. The PVTOL is a mathematical model of a flying object that evolves in a vertical plane [8]. It has three degrees of freedom (x,y, and θ) corresponding to its position and orientation in the plane. The PVTOL is composed of two thrusters that produce a force and a moment on the flying vehicle. It is an underactuated system since there are three degrees of freedom and only two inputs [8].

The four-rotor quadcopter can reduce to a PVTOL problem by set roll and yaw angle to zero. It can be seen as two PVTOL connected such that their axes are orthogonal.

3.1.1 Altitude and Yaw Control

The control of the vertical position can be obtained by

$$u = (r_1 + mg)\frac{1}{\cos\theta\cos\phi} \quad (3.1)$$

$$\text{Where } r_1 = -a_{z1}\dot{z} - a_{z2}(z - z_d) \quad (3.2)$$

Where a_{z1} and a_{z2} are positive constants. Z_d is desired altitude.

Yaw angular position can be controlled by

$$\tilde{\tau}_\psi = -a_{\psi 1}\dot{\psi} - a_{\psi 2}(\psi - \psi_d) \quad (3.3)$$

Substitute (3.1) ~ (3.3) back to (2.29) ~ (2.34), we can have

$$m\ddot{x} = -(r_1 + mg)\frac{\tan\theta}{\cos\phi} \quad (3.4)$$

$$m\ddot{y} = (r_1 + mg)\tan\phi \quad (3.5)$$

$$\ddot{z} = \frac{1}{m}(-a_{z1}\dot{z} - a_{z2}(z - z_d)) \quad (3.6)$$

$$\ddot{\psi} = -a_{\psi 1}\dot{\psi} - a_{\psi 2}(\psi - \psi_d) \quad (3.7)$$

$$\ddot{\theta} = \tilde{\tau}_\theta \quad (3.8)$$

$$\ddot{\phi} = \tilde{\tau}_\phi \quad (3.9)$$

The control parameters $a_{z1}, a_{z2}, a_{\psi 1}, a_{\psi 2}$should be carefully chosen to ensure a stable well-damped response in vertical and yaw axes [8].

From (3.6) to (3.7), it follows $\psi \to \psi_d$ and $z \to z_d$.

3.1.2 Roll Control

From (3.2) and (3.6) $r_1 \to 0$. Therefore, for a time T large enough, r_1 and ψ are arbitrary small and (3.4), (3.5) can reduce to

$$\ddot{x} = -g\frac{\tan\theta}{\cos\phi} \qquad (3.10)$$

$$\ddot{y} = g\tan\phi \qquad (3.11)$$

By the observation, we discovered that the subsystem (3.11), (3.9) is easier to deal with. And the nonlinear control based on nested saturations is first introduced here. This type of control allows in the limit a guarantee of arbitrary bounds for $\phi, \dot{\phi}, y \; and \; \dot{y}$ [8]. To further simplify the subsystem, we will impose a very small upper bound on $|\phi|$such that $\tan\phi \approx \phi$.

Finally, the subsystem is reduced to

$$\ddot{y} = g\phi \qquad (3.12)$$

$$\ddot{\phi} = \tilde{\tau}_\phi \qquad (3.13)$$

Which represents four integrators in cascade. And using the technique presented in [9], the controller can be designed by

$$\tilde{\tau}_\phi = -\sigma_{\phi 1}\left(\dot{\phi} + \sigma_{\phi 2}\left(\phi + \dot{\phi} + \sigma_{\phi 3}\left(2\phi + \dot{\phi} + \frac{\dot{y}}{g} + \sigma_{\phi 4}\left(\dot{\phi} + 3\phi + 3\frac{\dot{y}}{g} + \frac{y}{g}\right)\right)\right)\right)$$

(3.14)

Also with respect to the result in [9], we can prove the $\phi, \dot{\phi}, y, \dot{y}$ converge to zero.

3.1.3 Pitch Control

As $\phi \to 0$, from (3.10) we can get another simplified subsystem as

$$\ddot{x} = -g \tan\theta \qquad (3.15)$$

$$\ddot{\theta} = \tilde{\tau}_\theta \qquad (3.16)$$

Using the same idea that $\tan\theta \approx \theta$, the subsystem reduced to

$$\ddot{x} = -g\theta \qquad (3.17)$$

$$\ddot{\theta} = \tilde{\tau}_\theta \qquad (3.18)$$

Similarly, the controller is designed as

$$\tilde{\tau}_\theta = -\sigma_{\theta 1}\left(\dot{\theta} + \sigma_{\theta 2}\left(\theta + \dot{\theta} + \sigma_{\theta 3}\left(2\theta + \dot{\theta} + \frac{\dot{x}}{g} + \sigma_{\theta 4}\left(\dot{\theta} + 3\theta + 3\frac{\dot{x}}{g} + \frac{x}{g}\right)\right)\right)\right)$$

(3.19)

And, we can prove the $\theta, \dot{\theta}, x, \dot{x}$ converge to zero.

3.2 Simulation

3.2.1 Simulation Specification

In this section, we are going to determine the model and the parameters specifications for the simulation. First, we have the generalized model (2.36) deducted from chapter two. Next, we have four inputs (3.1), (3.3), (3.14), (3.19) designed in chapter three to be applied to the simulation.

For the parameters, they are depend on the real quadcopter we wanted to simulate. In this case we will use the quadcopter I built before as it showed in figure 1.1. Most of the parameters, like the mass m, length of the arms l, can be measured directly.

Parameters	Values	Unites
Weight/m	520	g
g	9.81	m/s^2
l	20.5	cm
Height	11	cm
Maximum Length	76	cm
Propeller Blade Length	20	cm
I_{xx}	$7.5x10^{-3}$	Kg/m^2
I_{yy}	$7.5x10^{-3}$	Kg/m^2
I_{zz}	$1.2x10^{-3}$	Kg/m^2

Table 3.1 Parameters of Quadcopter

The four control signals are transmitted by transmitter named ASHDS radio. The four control signals are referred as throttle control input u, pitch control input $\tilde{\tau}_\theta$, roll control input $\tilde{\tau}_\phi$, and yaw control put $\tilde{\tau}_\psi$. These control signals are constrained in the boundary to satisfy

$$0.65[V] < u < 4.70[V]$$

$$1.25[V] < \tilde{\tau}_\theta < 4.15[V]$$

$$0.75[V] < \tilde{\tau}_\phi < 4.50[V]$$

$$0.40[V] < \tilde{\tau}_\psi < 4.15[V]$$

(3.20)

And for the numerical parameters in u and $\tilde{\tau}_\theta$, and the saturation boundaries in $\tilde{\tau}_\phi$, $\tilde{\tau}_\psi$, are selected using following procedure.

The yaw controller is basically a PD controller. The parameters are selected to get a short settling time without having small oscillations in the yaw displacement.

For the parameters of roll control, we first select the gain concerning roll angular velocity $\dot{\phi}$. Due to the on board gyro scope, the gain is relatively small. Next we select the controller gain concerning the roll displacement ϕ. We expect the roll error to converge to zero fast and also with fewer oscillations. As for the $\dot{y}$ and the amplitude of the saturation function are selected to make the quadcopter reduces its speed in the y axis fast enough. Finally for the gains regarding the y displacement, we have to adjust to obtain a satisfactory performance.

Due to the symmetry properties of quadcopter, the choosing of the parameter according to the pitch control shares the same idea as before.

Therefore, we choose the parameters as:

Phase	Control Parameter	Value
Altitude	a_{z1}	0.001
	a_{z2}	0.002
Yaw Control	$a_{\psi 1}$	2.4
	$a_{\psi 2}$	0.08
Roll Control	M_{ϕ_1}	2
	M_{ϕ_2}	1
	M_{ϕ_3}	0.2
	M_{ϕ_4}	0.1
Pitch Control	M_{θ_1}	2
	M_{θ_2}	1
	M_{θ_3}	0.2
	M_{θ_4}	0.1

Table 3.2 Control Parameters Choosing

3.2.2 Simulation Result

Based on the simulation set up, with the initial condition with (1,1,1,1,1,1,1,1,1,1,1,1) we have $x, y, z, \psi, \theta, \phi$ of the quadcopter showed as:

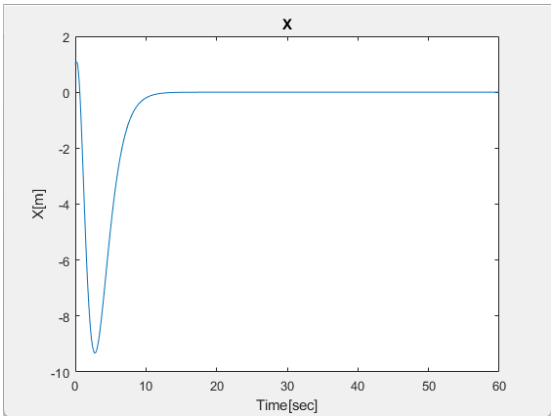

Figure 3.1 Position X

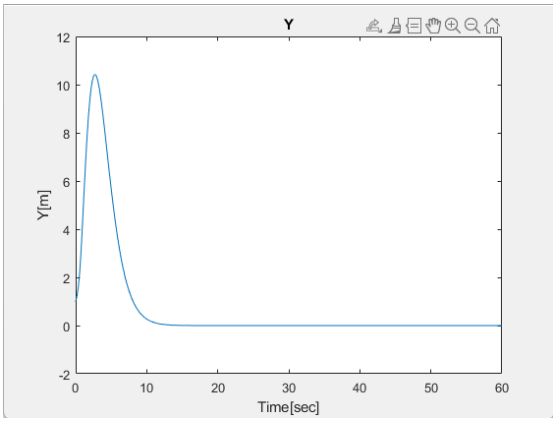

Figure 3.2 Position Y

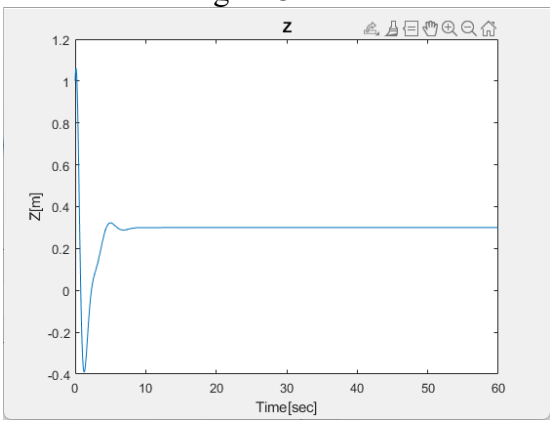

Figure 3.3 Position Z

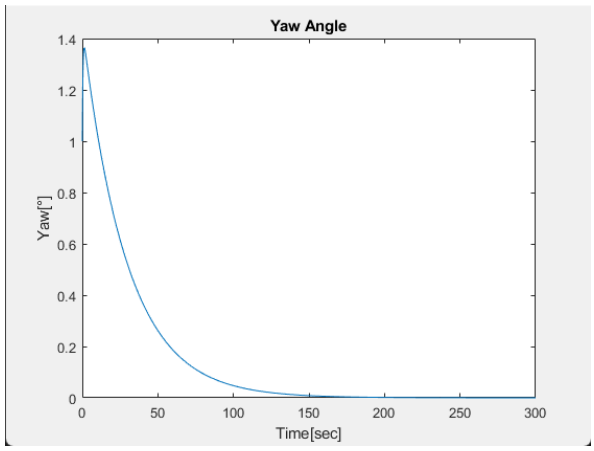

Figure 3.4 Yaw Angle

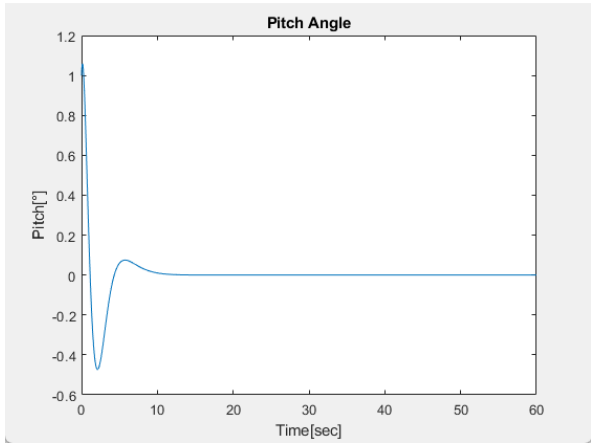

Figure 3.5 Pitch Angle

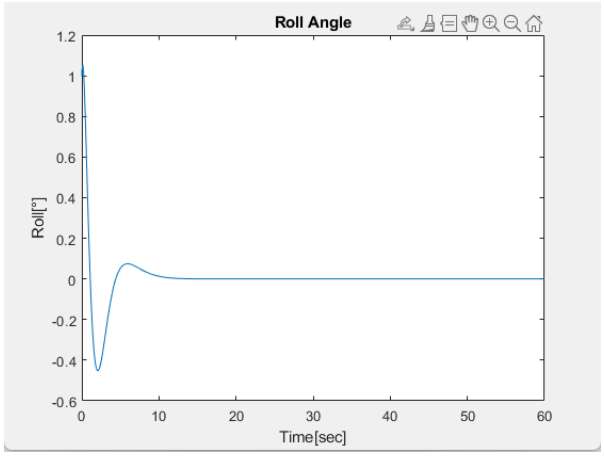

Figure 3.6 Roll Angle

And we have a 3D motion of quadcopter showed as:

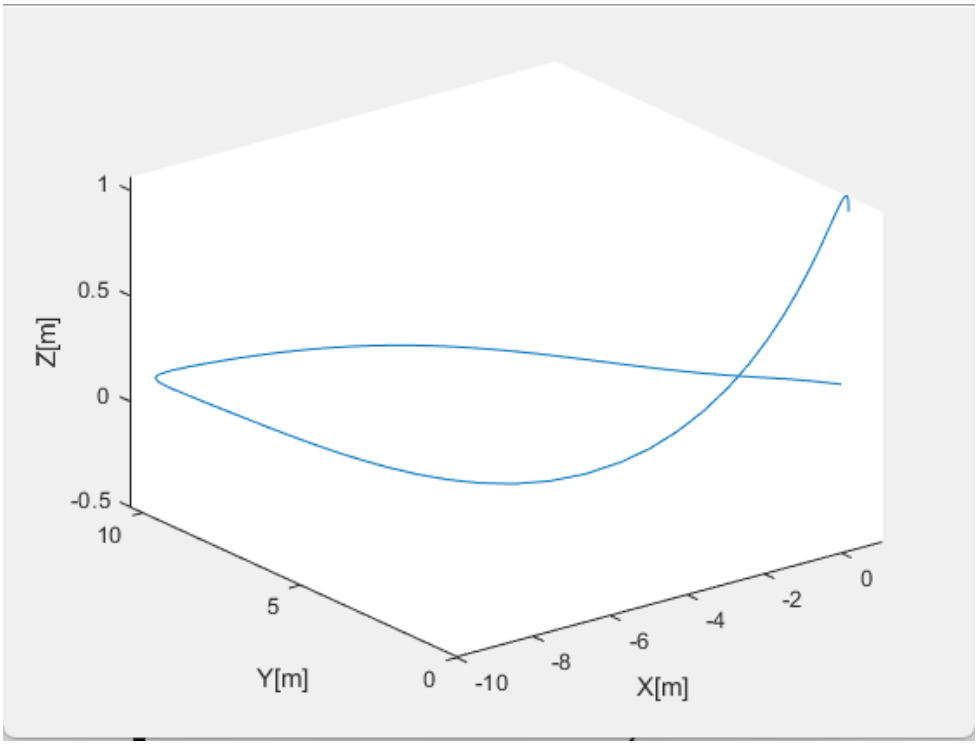

Figure 3.7 3D motion of quadcopter starting with (1,1,1)

As we can see, the first stage of controller which is Yaw and Attitude control, has a settling time which is less than 8 seconds. And the Roll and Pitch control can also settle in 10 seconds. The graphs shows a satisfactory result that all the states of quadcopter is successfully stabilized by the saturation controller with an acceptable range and time.

3.2.3 Disturbance Rejection

In this case we add disturbance signal to the system.

$$d_x(t) = \begin{cases} d1, & 5 \le t < 6 \\ 0, & t < 5 \; and \; t \ge 6 \end{cases} \quad (4.21)$$

$$d_y(t) = \begin{cases} d2, & 5 \le t < 6 \\ 0, & t < 5 \; and \; t \ge 6 \end{cases} \quad (4.22)$$

$d_x(t)$ is added to the state equation $\dot{x_1}$ and $d_y(t)$ is added to the state equation $\dot{x_2}$. This simulates a wind disturbance of $d1 \ m/s$ for 1 second on the direction of x and $d2 \ m/s$ for 1 second on y axis.

In this case, first we tried little disturbance, like $d1 = 1$ and $d2 = 2$. Its influence on the translational coordinates and rotational coordinate is not very significant. So we put a larger number, with $d1 = 5$ and $d2 = 6$. And the result is showed from figure 3.8-3.13.

By taking a look at the graphs, we can see all the them can restabilized after the disturbance with the time around 10 seconds. It could explain in two perspectives. First the system is easy to be stabilized. Second, under the controller we designed, the quadcopter can resist the external disturbance like the instant side wind.

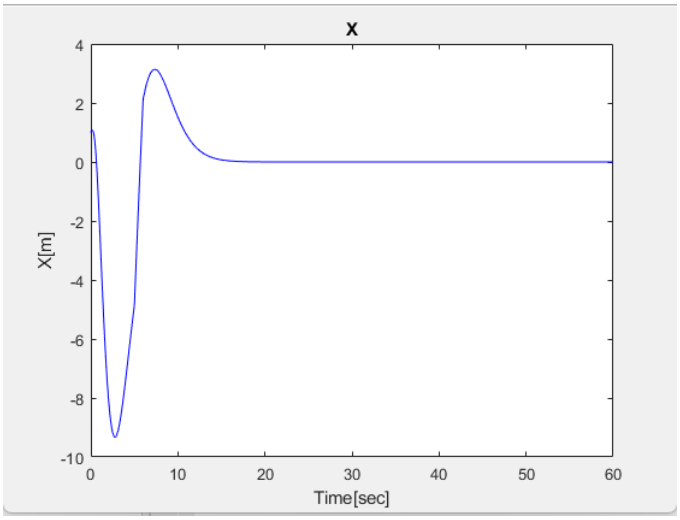

Figure 3.8 Position X (With Disturbance)

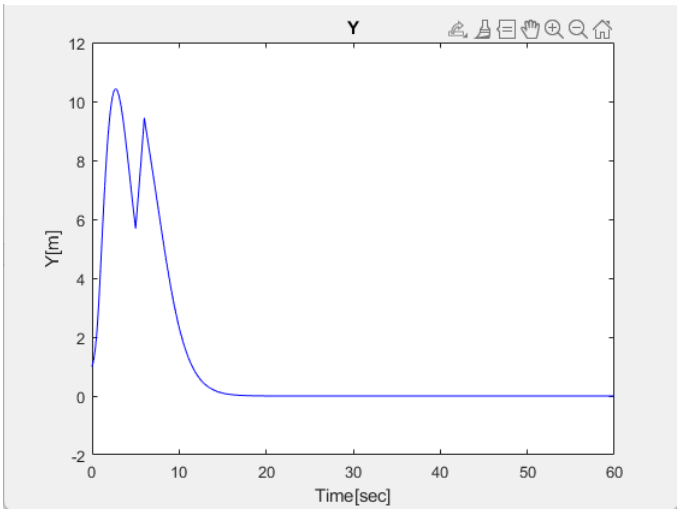

Figure 3.9 Position Y (With Disturbance)

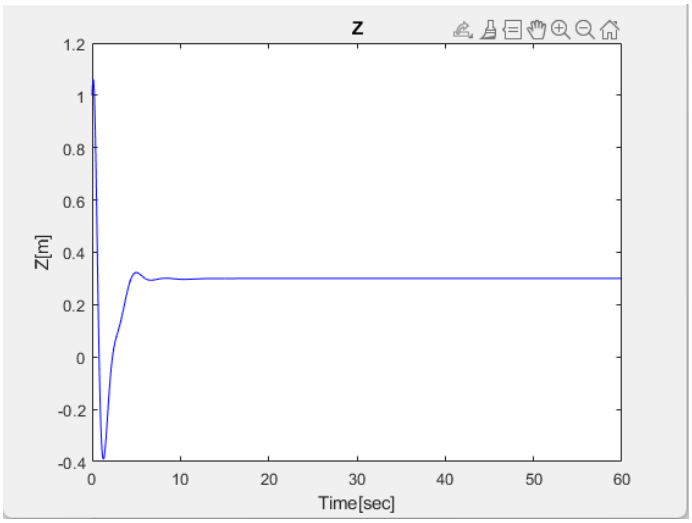

Figure 3.10 Position Z (With Disturbance)

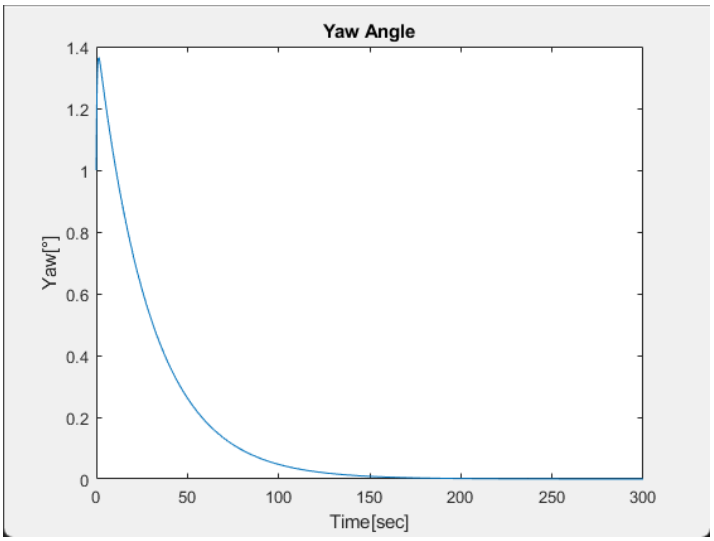

Figure 3.11 Yaw Angle (With Disturbance)

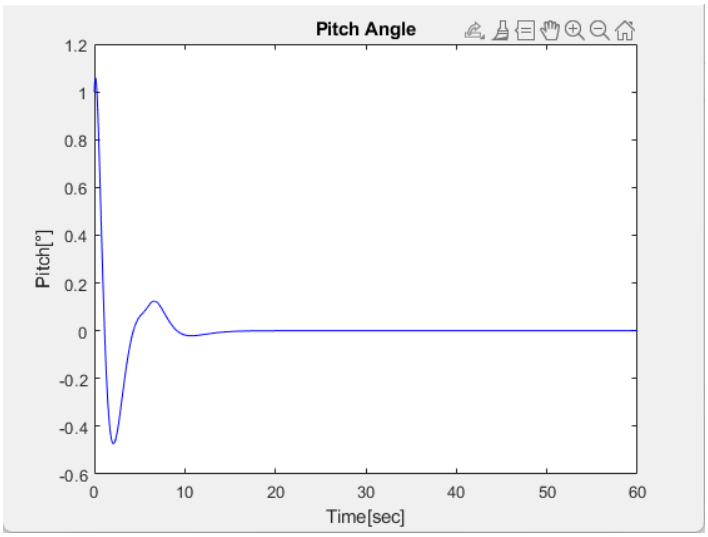

Figure 3.12 Pitch Angle (With Disturbance)

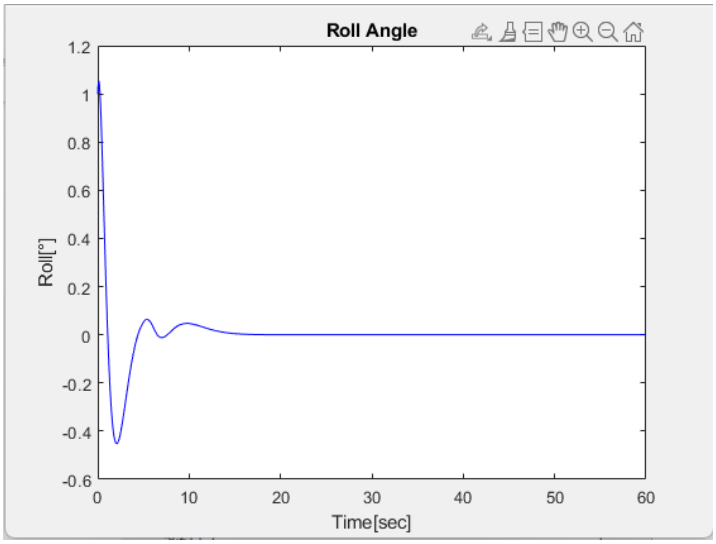

Figure 3.13 Roll Angle (With Disturbance)

3.3 Nested Saturation Application on PVTOL Model with Input Delays

The nested saturation control method can work perfectly for a standard four-propeller quadcopter. However, there are other UAVs, such as F-16 aircraft. Can the saturation design idea be applied to them?

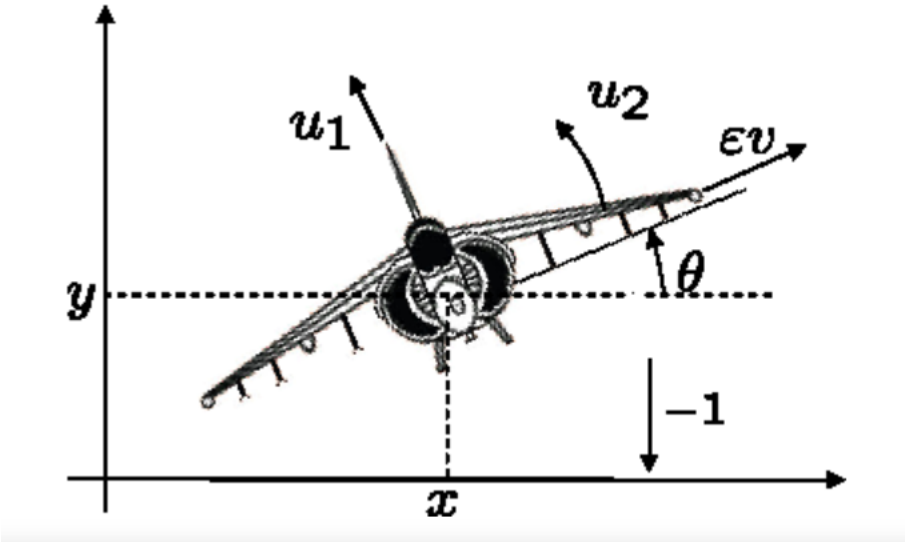

Figure 3.14 The PVTOL aircraft

Consider a simple PVTOL model showed in figure 3.8.

The dynamics are modelled and simplified by [11]

$$\ddot{x} = -u_1 \sin\theta$$

$$\ddot{y} = u_1 \cos\theta$$

$$\ddot{\theta} = u_2$$

(3.23)

Where x and y denote the center of mass, horizontal and vertical position and θ is the roll angle of the aircraft [11]. The control input is the thrust directed out the bottom of the aircraft, and they are non-negative by nature [13].

Based on the results presented in Teel [9] and the similar idea in chapter 3, the approach based on the use of non-linear combinations of linear saturation functions bounding the thrust input and the rolling moment to arbitrary saturation limits is introduced in R.Lozano's (2003) result [11]. By taking their simulation result, we can see that the same control idea can also perform well in the PVTOL case.

In Mazenc's (2007) [12] research for the same PVTOL model with delay in the input showed as

$$x_1 \doteq x_2$$

$$\dot{x_2} = u_1(t - \tau_1)\sin\theta$$

$$\dot{y_1} = y_2$$

$$\dot{y_2} = u_1(t - \tau_1)\cos\theta - 1$$

$$\dot{\theta} = \omega$$

$$\dot{\omega} = u_2(t - \tau_2)$$

(3.24)

The results show that bounded state feedback can achieve the global uniform asymptotic and local exponential stabilization of the model with two delayed inputs. Also, they showed how the presence of delays in inputs could be exploited to achieve the global

uniform asymptotic and local exponential stabilization of the PVTOL model when the variables of velocity are not measured [12].

In conclusion, besides the traditional PID control idea, the nested saturation control could also have the possibility to be wildly used in other UAVs. Also, with proper design, the saturation controller can make the system global asymptotic with parameter uncertainty.

4 Controlling Quadcopter with One, Two or Three Propellers Lost

4.1 Strategy of Balancing with Propellers Lost

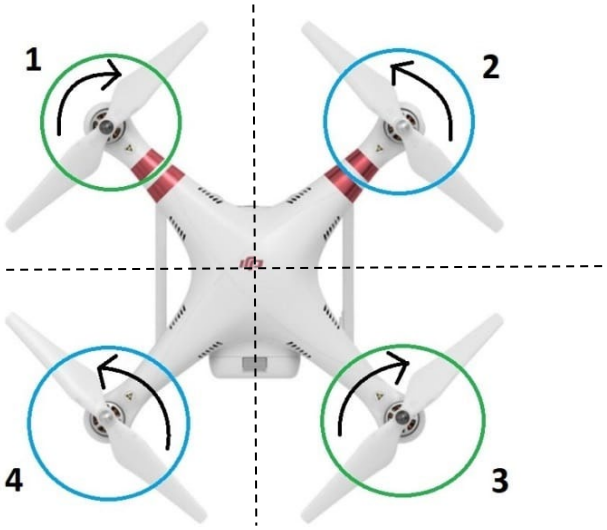

Figure 4.1 A example of DJI Drone

Generally, we use four propellers to control the quadcopter. However, when the quadcopter loses the power of propellers while it is going on a mission, losing one propeller is respect to losing one control input. In this situation, what is the solution of letting quadcopter fly properly?

There are three cases where one, two, or three propellers are lost. By intuitive thinking, if a quadcopter loses one of the propellers can still fly because there are still three propellers that can generate drag torque. In the case of losing two propellers, there are two different situations. Using the example of the DJI Drone shown in Figure 4.1, it cannot fly if two adjacent propellers (1 and 2) lose power because the net force generated

by the rest of the propellers is not centered at the middle point. However, if one pair of opposing propellers loses power, another pair can still generate net force at the center of mass. It can still be balanced if we are in a space completely free from outside influences, and the quadcopter is entirely symmetrical. There is a different way of quadcopter model design in the actual world experiment that could help the drone be balanced with two propellers only. At last, there is no way that the drone can still fly with three propellers lost.

This chapter will discuss the simple case of a quadcopter hovering in space with propellers lost. When the quadcopters lose various numbers of propellers, the resultant forces and torques acting on the vehicle are not likely to be zero. Therefore, the Strategy for controlling the quadcopters with actuators failure is to find the periodic solutions and equilibria, which allows the quadcopters to rotate with a constant angular velocity.

4.2 Angular Velocity Notation Model

From chapter 2, we have a six dimensional model that can fully control the quadcopter. The four control inputs $u, \tilde{\tau}_\psi, \tilde{\tau}_\theta, \tilde{\tau}_\phi$ (2.20) (2.22) are all based on the thrust force of each motor, or further considering as the angular speed of motors. Therefore, our first step is to find the relationship between angular velocity and the propellers' drag force or the motors' angular speed.

In this propellers lost quadcopter hovering study, we consider the propellers and the body of quadcopter separately as five independent rigid bodies. And there are five forces act on the vehicle: the weight mg, and the four propeller forces of magnitude f_i (2.7) which act in the body fixed direction $z = (0,0,1)$. Also there are five torques act on the vehicle: one for each propellers τ_{M_i} (Defined in 2.22) and a drag torque $\tau_d = (\tau_{d_x}, \tau_{d_y}, \tau_{d_z})$.

In (2.2) we have $\xi = (x, y, z) \in R^3$ which represents the quadcopter's center of mass.

Therefore the translational dynamics is represented as

$$m\ddot{\xi} = Rz \sum_{i=1}^{4} f_i + mg \qquad (4.1)$$

The body inertia tensor is still represented as

$$I^B = \begin{bmatrix} I_{xx}^B & 0 & 0 \\ 0 & I_{yy}^B & 0 \\ 0 & 0 & I_{zz}^B \end{bmatrix} \qquad (4.2)$$

The propeller is considered symmetric about its axis of rotation. Therefore its rotational inertia expressed in the quadcopter fixed frame is independent of the orientation of the propeller, and it is

$$I^P = \begin{bmatrix} I_{xx}^P & 0 & 0 \\ 0 & I_{xx}^P & 0 \\ 0 & 0 & I_{zz}^P \end{bmatrix} \qquad (4.3)$$

And the total inertias would be

$$I^T = 4 \cdot I^P + I^B = \begin{bmatrix} I_{xx}^B + 4I_{xx}^P & 0 & 0 \\ 0 & I_{yy}^B + 4I_{xx}^P & 0 \\ 0 & 0 & I_{zz}^B + I_{zz}^P \end{bmatrix} = \begin{bmatrix} I_{xx}^T & 0 & 0 \\ 0 & I_{yy}^T & 0 \\ 0 & 0 & I_{zz}^T \end{bmatrix} (4.4)$$

By [10] and definition of angular velocity (2.7) , the differential equation of body's angular velocity is

$$I^B \dot{v^B} + \sum_{i=1}^4 I^P \dot{v^{p_i}} + [\![v^B \times]\!] \left(I^B v^B + \sum_{i=1}^4 I^P (v^B + v^{p_i}) \right) = \tau_{total} \ (4.5)$$

On the left hand side, the first and second term represent the time derivative of the body rates and propeller speeds

$$I^B \dot{v^B} = (I_{xx}^B \dot{p}, I_{yy}^B \dot{q}, I_{zz}^B \dot{r}) \qquad (4.6)$$

$$I^P \dot{v^{p_i}} = (0,0, I_{zz}^P \dot{\omega_i}) \qquad (4.7)$$

And the third term is the cross-coupling term of the angular momentum due to taking the derivative in a non-inertial frame. Multiplying out the term we get

$$[\![v^B \times]\!] \left(I^B v^B + \sum_{i=1}^4 I^P (v^B + v^{p_i}) \right) = \begin{bmatrix} \left(I_{zz}^T - I_{yy}^T \right) qr + I_{zz}^P q \omega_t \\ -(I_{zz}^T - I_{xx}^T) qr - I_{zz}^P q \omega_t \\ \left(I_{yy}^T - I_{xx}^T \right) pq \end{bmatrix} (4.8)$$

With $\omega_t = \sum_{i=1}^4 \omega_i$ which is the sum of motor speeds.

The term τ_{total} on the right hand side of (4.5) represents all the moments acting on the body which include torques produced by motors and the moments due to the rotor forces.

$$\tau_{total} = \begin{bmatrix} (f_2 - f_4)l + \tau_{d_x} \\ (f_3 - f_1)l + \tau_{d_y} \\ \tau_1 + \tau_2 + \tau_3 + \tau_4 + \tau_{d_z} \end{bmatrix} \qquad (4.9)$$

By (2.21), we have the relationship between propellers' thrust force and the motor speed. And there is a strong linear relationship between the its torque and thrust force which is:

$$\tau_i = (-1)^{i+1} k_\tau f_i \qquad (4.10)$$

Where the coefficient k_τ is the sign given by the sense of rotation.

As for the term $\tau_d = (\tau_{d_x}, \tau_{d_y}, \tau_{d_z})$, since we are discussing the hovering problem, so we assume that the quadcopter acts only to oppose the yaw rate, with the proportionality constant γ :

$$\tau_d = (0,0,-\gamma r) \qquad (4.11)$$

For the last part of simplification, we assume that the motor speed is unaffected by the vehicle motion. Therefore, $I^P \ll I^B$ and $I^P v\dot{p}_\iota$ can be neglected.

Also using the same idea as we discussed before for the propeller disc's symmetry feature, the quadcopter is also symmetric that $I^B_{xx} = I^B_{yy}$.

With all the assumptions and simplifications, the equation (4.5) can be written as:

$$I^B_{xx}\dot{p} = k_f(\omega_2^2 - \omega_4^2)l - (I^T_{zz} - I^T_{xx})qr - I^P_{zz}q(\omega_1 + \omega_2 + \omega_3 + \omega_4) \qquad (4.12)$$

$$I^B_{xx}\dot{q} = k_f(\omega_3^2 - \omega_1^2)l - (I^T_{zz} - I^T_{xx})pr - I^P_{zz}p(\omega_1 + \omega_2 + \omega_3 + \omega_4) \qquad (4.13)$$

$$I^B_{zz}\dot{r} = -\gamma r + k_\tau k_f(\omega_1^2 - \omega_2^2 + \omega_3^2 - \omega_4^2) \qquad (4.14)$$

In the end, as we discussed in chapter 2, the standard quadcopter model allows us for control its full attitude R to the desired attitude. In this propeller lost quadcopter hovering case, we only consider a single direction of attitude, which refers to a reduced attitude kinematics.

The differential equation of a unit vector stationary in the inertial frame but expressed in body frame as $n = (n_x, n_y, n_z)$ is expressed by the cross product

$$\dot{n} = -v^B \times n \qquad (4.15)$$

4.3 Equilibria and Desired Trajectory of Quadcopter Maintaining Hovering Status

This section presents the solutions for the desired position and attitude of quadcopter with propellers lost. And we are specifically focusing on loss of one and two (opposing) propellers because when three propellers lost, the system is not controllable with only one input.

The goal is to find the periodic solution $\overline{n} = (\overline{n}_x, \overline{n}_y, \overline{n}_z)$ with constant angular velocity $\overline{v}^B$. From (4.9), it is required that $\dot{\overline{n}} = 0$ and the properties of the cross product follows that

$$\overline{n} = \epsilon \overline{v}^B \qquad (4.16)$$

With norm constraint on n as

$$\|\overline{n}\| = \left\|\epsilon \overline{v}^B\right\| = 1 \qquad (4.17)$$

The primary axis is pointing opposite to the gravity along the periodic solution, and it is required that there is no acceleration for the quadcopter in the direction of the gravity. Therefore

$$\overline{f_t}\overline{n}_z = \left(\overline{f_1} + \overline{f_2} + \overline{f_3} + \overline{f_4}\right)\overline{n}_z = m\|g\| \qquad (4.18)$$

If $\overline{n_z} < 1$, it means there is a part of total thrust force perpendicular to the gravity which could result into an acceleration in this direction. In this case, the vehicle will move along a horizontal circular trajectory with a period of [3]

$$T_c = \frac{2\pi}{\left\|\overline{v}^B\right\|} \qquad (4.19)$$

And a radius of

$$\overline{R}_c = \frac{\sqrt{1-\overline{n}_z{}^2}}{\overline{n}_z}\frac{\|g\|}{\left\|\overline{v}^B\right\|^2} \qquad (4.20)$$

To solve the trajectory for each cases, there are in total of eleven unknowns to solve:

$$\overline{n}_x, \overline{n}_y, \overline{n}_z, \overline{p}, \overline{q}, \overline{r}, \epsilon, \overline{\omega}_1, \overline{\omega}_2, \overline{\omega}_3, \overline{\omega}_4$$

by utilizing (4.6)-(4.8) (with angular accelerations set to zero) and (4.9)-(4.11).

Due to the symmetry property of quadcopter, the equilibrium yaw rate is independent of pitch and roll rates and can be solved independently as

$$\overline{r} = \frac{k_\tau k_f}{\gamma}\left(\overline{\omega}_1^2 - \overline{\omega}_2^2 + \overline{\omega}_3^2 - \overline{\omega}_4^2\right) \qquad (4.21)$$

In the next two subsections we will discuss the solution for one propeller and two opposing propellers lost. Each lost propeller will add a constraint of the form $\omega_i = 0$.

4.3.1 Solution if One Propeller Loses

Choose propeller 4 has failed, then $\overline{f_4} = \overline{\tau}_4 = \overline{\omega}_4 = 0$. In this case, an intuitive way of specifying the unknown terms is two suppose the opposing propellers 1 and 3 to produce equal thrust that $\overline{f_1} = \overline{f_3}$, and choose a ratio $\rho = \frac{\overline{f_2}}{\overline{f_1}}$ which is also defined as a tuning factor. This design reduces the unknowns from eleven to seven.

From (4.13), one solution is $\overline{p} = 0$ and $\overline{n}_x = 0$ for all choice of ρ. For small ρ, as ρ grows, $\overline{n}_z$ decreases and the total force in (4.18) increases.

The radius $\overline{R}_c$ of horizontal orbit (4.20) will be zero at ρ = 0. But the relationship between the angular velocity and ρ is harder to predict.

4.3.2 Solution if Two Propellers Lose

Assume propellers 2 and 4 are failed. Then $\overline{\omega}_2 = \overline{\omega}_4 = 0$ and it leaves one degree of freedom. To balance the quadcopter, we consider $\overline{\omega}_1 = \overline{\omega}_3$. The equilibrium can now be solved as

$$\overline{f_1} = \overline{f_3} = \frac{1}{2} m \|g\| \qquad (4.22)$$

$$\overline{\omega}_1 = \overline{\omega}_3 = -\sqrt{\frac{m\|g\|}{2k_f}} \qquad (4.23)$$

$$\overline{v}^B = \left(0,0,\frac{k_\tau m\|g\|}{\gamma}\right) \qquad (4.24)$$

$$\overline{n} = (0,0,1) \qquad (4.25)$$

For the two-propeller case, the quadcopter will be stationary at a point in space and $\overline{R}_c = 0$.

4.4 Controllability

In this section, we are going to discuss the controllability for two cases. It is accomplished by exploiting the time invariant nature of attitude equilibria and do the linearization, the check the rank of the Controllability A.

Define the state vector $s = (p, q, n_x, n_y)$ to describe the reduced attitude. And its deviation from the equilibrium is written as $\tilde{s} = s - \overline{s}$ and it evolve to first order as [10]

$$\dot{\tilde{s}} = A\tilde{s} + Bu \tag{4.26}$$

Where

$$A = \frac{\partial \dot{s}}{\partial s} \; where \; s = \overline{s}, = \begin{bmatrix} 0 & \overline{a} & 0 & 0 \\ -\overline{a} & 0 & 0 & 0 \\ 0 & -\overline{n}_z & 0 & \overline{r} \\ \overline{n}_z & 0 & -\overline{r} & 0 \end{bmatrix} \tag{4.27}$$

And

$$\overline{a} = \frac{I_{xx}^T - I_{zz}^T}{I_{xx}^B}\overline{r} - \frac{I_{zz}^P}{I_{xx}^B}(\overline{\omega}_1 + \overline{\omega}_2 + \overline{\omega}_3 + \overline{\omega}_4) \tag{4.28}$$

And the input u enters the system through matrix B.

The definition of B and u for these two cases will be different and it depends on the number of remaining propellers.

4.4.1 Controllability of One Propeller Lost Case

In this case, the input vector $u = (u_1, u_2)$ is introduced as

$$u_1 = \left(f_3 - \overline{f}_3\right) - \left(f_1 - \overline{f}_1\right) \tag{4.29}$$

$$u_2 = \left(f_2 - \overline{f}_2\right) \tag{4.30}$$

And the total thrust has to match the desired thrust as:

$$f_1 + f_2 + f_3 = \overline{f}_1 + \overline{f}_2 + \overline{f}_3 \tag{4.31}$$

Now the system (4.26) can be expand as

$$\dot{\tilde{s}} = A\tilde{s} + B_{(3)}u \tag{4.32}$$

$$B_{(3)} = \frac{l}{I_{xx}^B}\begin{bmatrix} 0 & 1 \\ 1 & 0 \\ 0 & 0 \\ 0 & 0 \end{bmatrix} \tag{4.33}$$

Examining the rank of controllability matrix

$$C_{(3)} = [B_{(3)} \quad AB_{(3)} \quad A^2B_{(3)} \quad A^3B_{(3)}] \tag{4.34}$$

And it has full rank so that it is controllable if $l \neq 0, \overline{n}_z \neq 0$.

4.4.2 Controllability of Two Propellers Lost Case

In this case, the system has only one input u_1 showed in (4.23). And now the system is given by

$$\dot{\tilde{s}} = A\tilde{s} + B_{(2)}u \tag{4.35}$$

$$B_{(2)} = \frac{l}{I_{xx}^{B}}\begin{bmatrix}0\\1\\0\\0\end{bmatrix} \tag{4.36}$$

And total thrust still have to match the desired thrust

$$f_1 + f_3 = \overline{f}_1 + \overline{f}_3 \tag{4.37}$$

Now as for the controllability matrix $C_{(2)} = [B_{(2)} \quad AB_{(2)} \quad A^2B_{(2)} \quad A^3B_{(2)}]$, or equivalently if the determinant of $C_{(2)}$ is non-zero.

$$\overline{a}\,\overline{r}\,\overline{n}_z^2(\overline{a}+\overline{r})^2\left(\frac{l}{I_{xx}^{B}}\right)^4 \neq 0 \tag{4.38}$$

Combine with (4.18), assume $l \neq 0$, which leaves

$$\overline{a}\,\overline{n}_z^2(\overline{a}+\overline{r})^2 \neq 0 \tag{4.39}$$

By (4.25), $\overline{n}_z = 1$. Then the system is uncontrollable if $\overline{a} = 0$, or $(I_{xx}^{T} - I_{zz}^{T})\overline{r} = 2I_{zz}^{P}\overline{\omega}_1$which that the vehicle roll rate p is uncontrollable. If $\overline{a} + \overline{r} = 0$ pr $(I_{xx}^{T} + I_{xx}^{B} - I_{zz}^{T})\overline{r} = 2I_{zz}^{P}\overline{\omega}_1$, the linearized system has two uncontrollable modes corresponding to $p + \overline{a}\,\overline{n}_x$ and $\overline{n}_y$.

4.5 Tilting Design Approach

Several years ago, a video showed one of the authors in [3] named Raffaello D'Andrea flying a quadcopter across the arena with two of its propellers cut off. It seems to contradict our controllability test in section 4.4. However, there could be some model improvement based on the traditional one. For example, a tilting arm design has the potential to make the quadcopter still fly with two propellers failure.

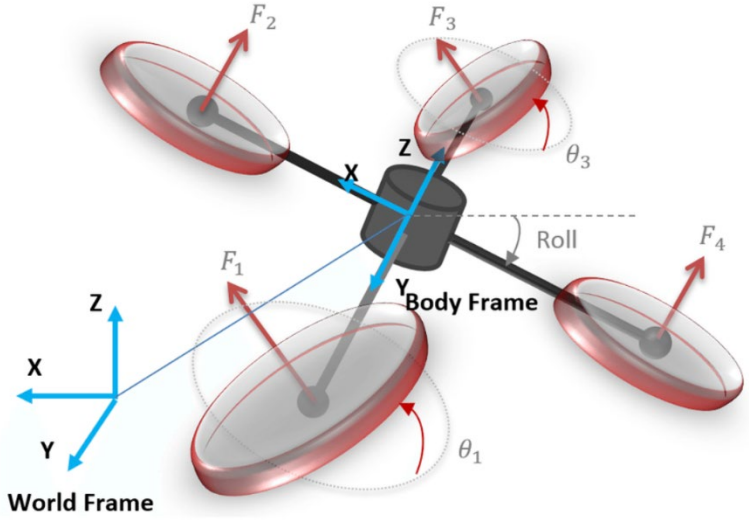

Figure 4.2 Coordinate system and forces acting on the tilting quadcopter

The design is accomplished by using additional motors to each rotor that enables the rotor to rotate along the axis of the quadcopter arm.

For the traditional model presented in chapter 2, the quadcopter is designed by having only four independent control inputs to control a six-dimensional position and orientation. In this tilting design, with more actuators installed, the under-actuated system turned into over-actuated system. It could allow us to have a complete control over the position and orientation [4].

Back to the case with propellers 1 and 3 disabled, by intuitive thinking, the quadcopter may still fly as it showed in Raffaello D'Andrea's experiment. Tilting the axis of propellers 2 and 4 could change the direction of drag force f_2 and f_4 because the design provides more DOF (Degree of Freedom) to the quadcopter. Consider the case that the axis with propellers 1 and 3 is sloping, changing the direction of f_2 and f_4 can pull the axis back to the horizontal position.

The tilting design provides more flexibility to the quadcopter. However, sometimes adding more actuators to the system means more power consumption. Therefore whether the value brought by this design is greater than its cost is worth exploring.

5 Conclusion

In this thesis, first, we have the dynamic model of the quadcopter obtained via a Lagrange approach and the control algorithm based on the nested saturation. The proposed strategy has been successfully applied to the quadcopter. Also, the simulation results have shown that the controllers perform satisfactorily. The saturation control idea is highly compatible with PVTOL models. It can also be applied to other UAVs, and it can deal with the situation when the system has parameter uncertainty.

As for the second part, we can see that when the quadcopter loses two or three propellers, the system is not controllable. However, while it lost one propeller, the system is still controllable. Furthermore, we can find a periodic solution for the quadcopter to maintain the hovering flying state. Moreover, the trajectory is circular. On the other hand, adding more actuators to make the quadcopter's arms rotate could help the vehicle fly stabler with propellers disabled.

6 Future Study

6.1 Applying Nested Saturation Design Idea to other UAVs

In the real world, besides the quadcopter, there are a lot of different kinds of UAVs that are worth studying. The PVTOL models are prevalent in studies of all kinds of flying vehicles. Based on the control technique we have, we can apply the idea of nested saturation feedback to other vehicles, for example, helicopters and jet aircraft.

6.2 Improve the Physical Structure Design of Quadcopter

The four motors quadcopter is the most common model we can see in the market. However, improving the physical structure of the quadcopter allows the quadcopter to be more flexible and more functional. For example, adding two more rotors along the quadcopter axis can make the quadcopter fly with two propellers cut off. The drone is a very powerful tool in our daily life, and it is worth investigating.

References

[1] Gupte, Shweta, Paul Infant Teenu Mohandas, and James M. Conrad. "A survey of quadrotor unmanned aerial vehicles." 2012 Proceedings of IEEE Southeastcon. IEEE, 2012.

[2] Cai, Guowei, Jorge Dias, and Lakmal Seneviratne. "A survey of small-scale unmanned aerial vehicles: Recent advances and future development trends." Unmanned Systems 2.02 (2014): 175-199.

[3] Mueller, Mark W., and Raffaello D'Andrea. "Stability and control of a quadrocopter despite the complete loss of one, two, or three propellers." 2014 IEEE international conference on robotics and automation (ICRA). IEEE, 2014.

[4] Nemati, Alireza, and Manish Kumar. "Modeling and control of a single axis tilting quadcopter." 2014 American Control Conference. IEEE, 2014.

[5] Dydek, Zachary T., Anuradha M. Annaswamy, and Eugene Lavretsky. "Adaptive control of quadrotor UAVs: A design trade study with flight evaluations." IEEE Transactions on control systems technology 21.4 (2012): 1400-1406.

[6] Erginer, Bora, and Erdinc Altug. "Modeling and PD control of a quadrotor VTOL vehicle." 2007 IEEE Intelligent Vehicles Symposium. IEEE, 2007.

[7] Bouabdallah, Samir, and Roland Siegwart. "Backstepping and sliding-mode techniques applied to an indoor micro quadrotor." Proceedings of the 2005 IEEE international conference on robotics and automation. IEEE, 2005.

[8] Castillo, Pedro, Alejandro Dzul, and Rogelio Lozano. "Real-time stabilization and tracking of a four-rotor mini rotorcraft." IEEE Transactions on control systems technology 12.4 (2004): 510-516.

[9] Teel, Andrew R. "Global stabilization and restricted tracking for multiple integrators with bounded controls." Systems & control letters 18.3 (1992): 165-171.

[10] P. H. Zipfel, Modeling and Simulation of Aerospace Vehicle Dynamics Second Edition. AIAA, 2007.

[11] Zavala-Rio, Arturo, Isabelle Fantoni, and Rogelio Lozano. "Global stabilization of a PVTOL aircraft model with bounded inputs." International Journal of Control 76.18 (2003):1833-1844.

[12] Francisco, Rogelio, Frédéric Mazenc, and Sabine Mondié. "Global asymptotic stabilization of a PVTOL aircraft model with delay in the input." Applications of time delay systems. Springer, Berlin, Heidelberg, 2007. 343-356.

[13] Hauser, John, Shankar Sastry, and George Meyer. "Nonlinear control design for slightly non-minimum phase systems: Application to V/STOL aircraft." Automatica 28.4 (1992): 665-679.